Polymer Journal (2015) 47, 625–630

www.nature.com/pj

ORIGINAL ARTICLE

Synthesis of polyisocyanides bearing oligothiophene pendants: higher-order structural control through pendant framework design

Tomoyuki Ikai[1], Yugaku Takagi[1], Ken-ichi Shinohara[2], Katsuhiro Maeda[1] and Shigeyoshi Kanoh[1]

L-Alanine-based polyisocyanides bearing oligothiophene (OT) pendants (poly-3a and poly-3b) were synthesized and the influence of the OT pendants on the chiroptical properties and helix-forming abilities of the polymers was investigated. Poly-3a bearing a quinquethiophene unit with two *n*-hexyl chains successfully formed a preferred-handed helical conformation by simultaneous interactions of the OT-pendant π–π stacking and hydrogen bonding of the amide groups. In contrast, poly-3b, which possesses a branched alkyl chain on behalf of the terminal *n*-hexyl chain of poly-3a, did not form a higher-ordered helical conformation. The results suggest that the structure of the alkyl chains positioned far from the polymer backbones remotely and sensitively affected the ability of the polymer to form a helical conformation. We also found that the structure of the OT pendants significantly affect the molecular weight as observed by AFM measurements. The polyisocyanide poly-3c bearing a bithiophene unit was additionally synthesized to examine the influence of the number of thiophene rings within the OT pendants on the higher-order structure formation.
Polymer Journal (2015) **47,** 625–630; doi:10.1038/pj.2015.42; published online 10 June 2015

INTRODUCTION

Biomacromolecules including DNA, RNA and proteins show miraculous and varied functionality in relation to specific molecular recognitions and stereoselective catalytic activities, the expressions of which are closely related to the secondary structure (for example, helical conformations) of the biomacromolecules. These higher-order structures are constructed and stabilized by harmonious combination of noncovalent interactions (for example, coordination bonds, salt bridges, hydrogen bonding and π–π stacking interactions). By emulating the structural features of biomacromolecules, excellent functionalities are potentially provided to molecularly designed synthetic polymers. In fact, optically active synthetic polymers with defined helical conformations have been applied to chiral materials of interest,[1–8] and these often display improved performances when compared with their corresponding monomer and nonhelical polymer analogs. Polyisocyanides are recognized as one of the representative synthetic polymers capable of forming helical structures.[9,10] Among a wide variety of synthetic helical polymers reported so far,[6,8] polyisocyanides have a unique structural feature in that pendant units can be introduced to every carbon atom in the polymer backbone. Therefore, arbitrary functional pendants can be closely and helically arranged along the main chains, giving rise to distinctive macromolecular effects.

Polyisocyanides bearing optically active amino acid residues as pendants—termed polyisocyanopeptides—are reported to possess a preferred-handed helical conformation stabilized by intramolecular hydrogen bonding networks between the pendant amide linkages along the main chain.[11–13] On the basis of molecular modeling, vibrational circular dichroism (CD) and solid-state nuclear magnetic resonance (NMR) analyses, a main chain of polyisocyanopeptides is predicted to form an ~4/1 helical conformation, in which four repeating units constitute one helical turn and the helical handedness is dependent on the chirality of amino acid residues as pendant groups.[12,14,15] In addition, polyisocyanopeptides bearing electronically or optically functionalized pendants have great potential to be promising electron-, hole- or energy-transporting materials because of their densely packed pendant array. Actually, helical polyisocyanopeptides functionalized with polycyclic aromatic pendants, such as electron accepting perylenediimides[16–20] and electron donating carbazole,[21] have been utilized in semiconducting material applications.

Oligothiophenes (OTs) have been recognized as one of the most predominant organic semiconducting materials with an efficient hole-transport property, and used as a key component in various organic electronic devices,[22–25] such as organic photovoltaics, transistors and memories. The highly ordered arrangement of the OT units is very important for the enhanced performance of these devices. In this context, our research has focused on combining structural properties of polyisocyanopeptides with the functionality of the OT groups in order to create next-generation functional materials. In this work, we

[1]Graduate School of Natural Science and Technology, Kanazawa University, Kanazawa, Japan and [2]School of Materials Science, Japan Advanced Institute of Science and Technology (JAIST), Nomi, Japan
Correspondence: Professor T Ikai, Graduate School of Natural Science and Technology, Kanazawa University, Kakuma-machi, Kanazawa 920-1192, Japan.
E-mail: ikai@se.kanazawa-u.ac.jp
Received 23 March 2015; revised 10 May 2015; accepted 11 May 2015; published online 10 June 2015

have synthesized three novel polyisocyanopeptides (poly-**3a**–poly-**3c**) bearing OT pendants, and found that the frameworks of the incorporated OT pendants significantly affected the polymerization ability of the isocyanide monomer as well as the chiroptical properties and the helix-forming abilities. To the best of our knowledge, this is the first report on the synthesis of helical polyisocyanides bearing OT pendants.

EXPERIMENTAL PROCEDURE

Materials

The anhydrous solvents (dichloromethane (CH_2Cl_2), chloroform ($CHCl_3$), dimethyl sulfoxide, ethanol and tetrahydrofuran (THF)), the common organic solvents and 1-hydroxybenzotriazole were purchased from Kanto (Tokyo, Japan). Nickel(II) perchlorate hexahydrate ($Ni(ClO_4)_2{\cdot}6H_2O$) and 1-ethyl-3-(3-dimethylaminopropyl)carbodiimide hydrochloride (EDC-HCl) and trifluoroacetic acid were purchased from Wako (Osaka, Japan). Sodium hydrogen carbonate ($NaHCO_3$) was obtained from Kishida (Osaka, Japan). *N*-Formyl-L-alanine and *N*-methylmorpholine were purchased from Nacalai (Kyoto, Japan). Diphosgene and tetrabutylammonium bromide were from Aldrich (Milwaukee, WI, USA). Details on the synthesis of the ethylamine compounds bearing OT units (**1a**–**1c**) are described in Supplementary Scheme S1.

Monomer synthesis

*Synthesis of **2a**.* *N*-formyl-L-alanine (332 mg, 2.84 mmol) was added to a solution of **1a** (1.77 g, 2.83 mmol) and 1-hydroxybenzotriazole (417 mg, 3.12 mmol) in THF/dimethyl sulfoxide (2/1, v/v; 42 ml) and the mixture was cooled to 0 °C under a nitrogen atmosphere. To this mixture was added EDC-HCl (593 g, 3.12 mmol). After stirring at 0 °C for 8 h, the reaction system was diluted with CH_2Cl_2 and the solution was washed with saturated $NaHCO_3$ aqueous solution and brine and then dried over Na_2SO_4. After filtration, the solvent was removed by evaporation and the crude product was purified by silica gel chromatography using ethyl acetate as the eluent to give **2a** as an orange solid (1.91 g, 93% yield). ^{1}H NMR (500 MHz, $CDCl_3$, rt): δ 8.16 (s, 1H, CHO), 7.10–6.94 (m, 6H, Th-H), 6.93 (d, J = 4.0 Hz, 1H, Th-H), 6.79–6.69 (m, 2H, Th-H), 6.34–6.26 (brs, 1H, NH), 6.26–6.18 (brs, 1H, NH), 4.52 (quint, J = 7.2 Hz, 1H, NHC*H*CO), 3.62–3.49 (m, 2H, NHCH_2), 3.02 (t, J = 6.6 Hz, 2H, NHCH$_2$CH_2), 2.81 (t, J = 7.4 Hz, 2H, Th-CH$_2$), 2.71 (t, J = 7.7 Hz, 2H, Th-CH$_2$), 1.76–1.60 (m, 4H, 2Th-CH$_2$CH_2), 1.46–1.27 (m, 15H, NHCHCH_3, 6CH$_2$) and 0.97–0.83 (m, 6H, 2CH$_3$).

*Synthesis of **2b**.* The title compound **2b** was prepared from *N*-formyl-L-alanine and **1b** in the same way for **2a** and obtained in 95% yield as an orange solid. ^{1}H NMR (500 MHz, $CDCl_3$, rt): δ 8.15 (s, 1H, CHO), 7.08–6.95 (m, 6H, Th-H), 6.93 (d, J = 3.4 Hz, 1H, Th-H), 6.74 (d, J = 3.4 Hz, 1H, Th-H), 6.69 (d, J = 3.4 Hz, 1H, Th-H), 6.35–6.27 (brs, 1H, NH), 6.26–6.20 (brs, 1H, NH), 4.52 (quint, J = 7.0 Hz, 1H, NHC*H*CO), 3.62–3.46 (m, 2H, NHCH_2), 3.01 (t, J = 6.6 Hz, 2H, NHCH$_2$CH_2), 2.78–2.66 (m, 4H, Th-CH$_2$), 1.71-1.61 (m, 3H, Th-CH$_2$CH_2, CH$_2$CHCH$_2$), 1.45–1.16 (m, 41H, NHCHCH_3, 19CH$_2$) and 0.94–0.80 (m, 9H, 3CH$_3$).

*Synthesis of **2c**.* The title compound **2c** was prepared from *N*-formyl-L-alanine and **1c** in the same way for **2a** and obtained in 98% yield as a pale yellow solid. ^{1}H NMR (500 MHz, $CDCl_3$, rt): δ 8.14 (s, 1H, CHO), 6.91 (t, J = 2.9 Hz, 2H, Th-H), 6.70 (d, J = 3.4 Hz, 1H, Th-H), 6.66 (d, J = 3.4 Hz, 1H, Th-H), 6.37–6.25 (brs, 1H, NH), 6.24–6.12 (brs, 1H, NH), 4.51 (quint, J = 7.0 Hz, 1H, NHC*H*CO), 3.61–3.46 (m, 2H, NHCH_2), 2.99 (t, J = 6.6 Hz, 2H, NHCH$_2$CH_2), 2.78 (t, J = 7.4 Hz, 2H, Th-CH$_2$), 1.67 (quint, J = 7.8 Hz, 2H, Th-CH$_2$CH_2), 1.42–1.22 (m, 9H, NHCHCH_3, 3CH$_2$) and 0.89 (t, J = 6.6 Hz, 3H, CH$_3$).

*Synthesis of **3a**.* To a solution of **2a** (600 mg, 0.83 mmol) in CH_2Cl_2 (165 ml) was added *N*-methylmorpholine (0.36 ml, 3.3 mmol) and the mixture was cooled to − 40 °C under a nitrogen atmosphere. To this mixture was added a solution of diphosgene (0.055 ml, 0.45 mmol) in CH_2Cl_2 (5.4 ml) over a period of 1 h and the reaction was quenched by adding an aqueous saturated $NaHCO_3$ solution (5 ml). After vigorous stirring for 5 min, the resulting mixture was diluted with CH_2Cl_2 and washed with saturated $NaHCO_3$ aqueous solution and brine and then dried over Na_2SO_4. After filtration, the solvent was removed by evaporation and the crude product was purified by silica gel chromatography using CH_2Cl_2 as the eluent to give **3a** as an orange solid (419 mg, 71% yield). Mp: 138.1–138.5 °C. $[\alpha]_D^{25}$ +9.1 (*c* 1.0, $CHCl_3$). IR (KBr, cm^{-1}): 2140 (N≡C), 1667 (C=O). ^{1}H NMR (500 MHz, $CDCl_3$, rt): δ 7.07–7.00 (m, 5H, Th-H), 6.98 (s, 1H, Th-H), 6.93 (d, J = 4.0 Hz, 1H, Th-H), 6.78 (d, J = 3.4 Hz, 1H, Th-H), 6.73 (d, J = 3.4 Hz, 1H, Th-H), 6.64–6.55 (brs, 1H, NH), 4.25 (q, J = 7.1 Hz, 1H, NHC*H*C=O), 3.59 (q, J = 6.5 Hz, 2H, NHCH_2), 3.06 (t, J = 6.6 Hz, 2H, NHCH$_2$CH_2), 2.81 (t, J = 7.7 Hz, 2H, Th-CH$_2$), 2.71 (t, J = 7.7 Hz, 2H, Th-CH$_2$), 1.74–1.60 (m, 7H, 2Th-CH$_2$CH_2, NHCHCH_3), 1.47–1.24 (m, 12H, 6CH$_2$) and 0.94–0.86 (m, 6H, 2CH$_3$). ^{13}C NMR (125 MHz, $CDCl_3$, rt): δ 166.25, 161.36, 146.48, 139.85 (2C), 136.43, 136.18 (2C), 135.98, 135.65, 134.16, 133.28, 130.67, 126.70, 126.65, 125.66, 124.55, 124.43, 124.31, 124.26, 124.13, 123.79, 53.63, 41.18, 31.80, 31.70, 30.64, 30.28, 29.96, 29.48, 29.37, 28.94, 22.75, 22.72, 19.89 and 14.25. Calculated (Calcd) for $C_{38}H_{44}N_2OS_5{\cdot}H_2O$: C, 63.12; H, 6.41; N, 3.87. Found: C, 63.42; H, 6.32; N, 3.90.

*Synthesis of **3b**.* The title compound **3b** was prepared from **2b** in the same way for **3a** and obtained in 44% yield as an orange solid. Mp: 117.2–117.4 °C. $[\alpha]_D^{25}$ +7.5 (*c* 1.0, $CHCl_3$). IR (KBr, cm^{-1}): 2141 (N≡C), 1681 (C=O). ^{1}H NMR (500 MHz, $CDCl_3$, rt): δ 7.08–7.00 (m, 5H, Th-H), 6.98 (s, 1H, Th-H), 6.93 (d, J = 3.4 Hz, 1H, Th-H), 6.77 (d, J = 3.4 Hz, 1H, Th-H), 6.69 (d, J = 3.4 Hz, 1H, Th-H), 6.64–6.57 (brt, 1H, NH), 4.24 (q, J = 7.1 Hz, 1H, NHC*H*C=O), 3.59 (q, J = 6.5 Hz, 2H, NHCH_2), 3.06 (t, J = 6.6 Hz, 2H, NHCH$_2$CH_2), 2.77–2.68 (m, 4H, 2Th-CH$_2$), 1.72–1.61 (m, 5H, Th-CH$_2$CH_2, NHCHCH_3), 1.46–1.18 (m, 39H, 19CH$_2$, CH$_2$CHCH$_2$) and 0.95–0.81 (m, 9H, 3CH$_3$). ^{13}C NMR (125 MHz, $CDCl_3$, rt): δ 166.24, 161.35, 145.00, 139.84, 139.77, 136.46, 136.19, 136.17, 135.98, 135.62, 134.08, 133.50, 130.74, 126.71, 126.69, 125.64, 125.54, 124.43, 124.32, 124.26, 124.10, 123.80, 53.64, 41.18,

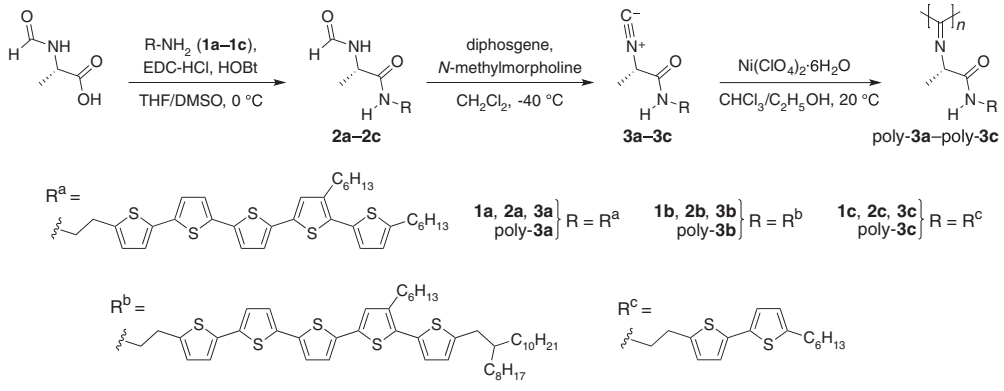

Scheme 1 Synthesis of polyisocyanides bearing oligothiophene pendants (poly-**3a**–poly-**3c**).

40.05, 34.60, 33.31, 32.06, 31.81, 30.63, 30.11, 29.96, 29.81, 29.77, 29.52, 29.50, 29.38, 26.73, 22.84, 22.76, 19.89, 14.28 and 14.26. Calcd for $C_{52}H_{72}N_2OS_5$: C, 69.28; H, 8.05; N, 3.11. Found: C, 69.33; H, 8.26; N, 3.09.

Synthesis of 3c. The title compound **3c** was prepared from **2c** in the same way for **3a** and obtained in 90% yield as a pale yellow solid. Mp: 103.9–104.1 °C. $[\alpha]_D^{25}$ +16.8 (*c* 1.0, $CHCl_3$). IR (KBr, cm^{-1}): 2143 (N≡C), 1667 (C=O). ^1H NMR (500 MHz, $CDCl_3$, rt): δ 6.92 (dd, *J* = 5.7, 3.4 Hz, 2H, Th-H), 6.73 (d, *J* = 3.4 Hz, 1H, Th-H), 6.65 (d, *J* = 3.4 Hz, 1H, Th-H), 6.62–6.53 (brt, 1H, NH), 4.23 (q, *J* = 7.1 Hz, 1H, NHC*H*C=O), 3.57 (q, *J* = 6.5 Hz, 2H, NHCH_2), 3.03 (t, *J* = 6.6 Hz, 2H, $NHCH_2CH_2$), 2.77 (t, *J* = 7.7 Hz, 2H, Th-CH_2), 1.71–1.62 (m, 5H, Th-CH_2CH_2, NHCHCH_3), 1.41–1.26 (m, 6H, $3CH_2$) and 0.88 (t, *J* = 6.9 Hz, 3H, CH_3). ^{13}C NMR (125 MHz, $CDCl_3$, rt): δ 166.22, 161.19, 145.42, 138.87, 137.07, 134.70, 126.44, 124.79, 123.27, 122.97, 53.64, 53.59, 41.18, 31.67, 30.25, 29.88, 28.86, 22.69, 19.87 and 14.22. Calcd for $C_{20}H_{26}N_2OS_2$: C, 64.13; H, 7.00; N, 7.48. Found: C, 63.97; H, 7.05; N, 7.43.

Polymerization

Polymerization of **3a–3c** was carried out according to Scheme 1 in a dry glass ampule using $Ni(ClO_4)_2{\cdot}6H_2O$ as a catalyst in a similar way as reported previously.[16] A typical polymerization procedure is described below.

To a solution of **3a** (50 mg, 71 μmol) in $CHCl_3$ (2.0 ml) was added $CHCl_3$–ethanol solution (50/1, v/v, 277 μl) containing $Ni(ClO_4)_2{\cdot}6H_2O$ (0.28 mg, 0.77 μmol). The solution was stirred at 20 °C until infrared spectrum revealed complete consumption of the monomer that was confirmed by the disappearance of the absorption peak ~2140 cm^{-1} based on the isocyanide group. The reaction mixture was poured into a large amount of ethanol and the resulting precipitate was collected by centrifugation to give the target polymer poly-**3a** as a red solid (48.6 mg, 97% yield). ^1H NMR (500 MHz, $CDCl_3$, rt): δ 7.13–6.45 (br, 9H, Th-H), 5.46–5.13 (br, 1H, CH), 3.77–3.27 (br, 4H, $NHCH_2CH_2$), 2.85–0.61 (br, 29H, alkyl-H). Analysis (Anal.) Calcd for $(C_{38}H_{44}N_2OS_5)_n$: C, 64.73; H, 6.29; N, 3.97. Found: C, 64.53; H, 6.38; N, 3.96.

In the same way, poly-**3b** and poly-**3c** were synthesized with the corresponding monomers. The polymerization results are summarized in Table 1.

Spectroscopic data of poly-3b. ^1H NMR (500 MHz, $CDCl_3$, rt): δ 9.86-7.90 (br, 1H, NH), 7.12–5.68 (br, 9H, Th-H), 5.67–4.57 (br, 1H, CH), 4.21–2.09 (br, 6H, Th-CH_2, $NHCH_2CH_2$) and 1.98–0.19 (br, 55H, alkyl-H). Anal. Calcd for $(C_{52}H_{72}N_2OS_5{\cdot}0.1H_2O)_n$: C, 69.14; H, 8.06; N, 3.10. Found: C, 68.90; H, 8.21; N, 3.09.

Spectroscopic data of poly-3c. ^1H NMR (500 MHz, $CDCl_3$, rt): δ 9.32–7.78 (br, 1H, NH), 7.02–5.94 (br, 4H, Th-H), 5.60–4.59 (br, 1H, CH), 4.26–2.21 (br, 4H, $NHCH_2CH_2$), 1.99–0.50 (br, 16H, alkyl-H). Anal. Calcd for $(C_{20}H_{26}N_2OS_2{\cdot}0.1H_2O)_n$: C, 63.82; H, 7.02; N, 7.44. Found: C, 63.53; H, 6.92; N, 7.35.

Molecular model

Before molecular dynamics (MD) simulation, the initial structure of a polymer chain model was generated at torsion angle of +70°, orientation of head to tail, degree of polymerization of 200 using the repeating unit. Sequentially, the geometry was optimized with the Dreiding force field and utilizing the Gasteiger partial charge calculation method.

MD simulations were carried out using the Forcite module of the BIOVIA Materials Studio (Dassault Systèmes BIOVIA, San Diego, CA, USA). Simulation in the NVT ensemble was conducted at 298K for 100 ps (time step of 0.5-fs, 200 000 steps) to equilibrate and relax a single chain of 200-mer of poly-**3a**. The Nose thermostat was used to control the temperature. After the equilibration, simulation in the NVE ensemble was conducted at 298K for 200 ps (time step of 1.0-fs, 200000 steps) as the sampling.

Table 1 Polymerization results of 3a–3c

Run	*Polymer*	*Yield (%)*[a]	*M_n (10^6)*[b]	*Mw/Mn*[b]	*λ_{max} (nm)*[c]
1	Poly-**3a**	97	1.9	2.8	431
2	Poly-**3b**	90	0.22	2.9	413
3	Poly-**3c**	83	0.10	1.5	316

[a]Ethanol (EtOH) insoluble part.
[b]Determined by size-exclusion chromatography (SEC; eluent: tetrahydrofuran (THF) containing 0.1 wt% tetrabutylammonium bromide (TBAB), polystyrene standards).
[c]Values from absorption spectra in chloroform ($CHCl_3$).

Analytical methods

The ^1H and ^{13}C NMR spectra were measured in $CDCl_3$ at room temperature with a JEOL ECA-500 spectrometer (JEOL, Tokyo, Japan). Infrared spectra were obtained using a JASCO FT/IR-460Plus spectrometer (JASCO, Tokyo, Japan) as a KBr pellet. The molecular weights and distributions of the polymers were estimated using size-exclusion chromatography equipped with a TSKgel α-M column (Tosoh, Tokyo, Japan), a JASCO PU-2080 Plus high-performance liquid chromatography pump and a JASCO UV-970 UV/VIS detector at 254 nm, where THF containing 0.1 wt% tetrabutylammonium bromide was used as the eluent. The molecular weight calibration curve was obtained with polystyrene standards (Tosoh). The optical rotation was measured at 25 °C with a JASCO P-1030 polarimeter. The UV–vis absorption and CD spectra were measured in $CHCl_3$ with 1.0 or 10 mm quartz cell using JASCO V-570 and JASCO J-720 spectrometers. A probe-scan-type atomic force microscope (AFM) (5500AFM, Agilent Technologies, Santa Clara, CA, USA) was used for molecular imaging in the dynamic (tapping) mode with a cantilever (OMCL-AC240TS, Olympus, Tokyo, Japan) having a spring constant of 1.7 N m^{-1} and resonance frequency of 70 kHz (typical values).[26] The set point was optimized for the gentle-touch imaging. A specimen for AFM imaging was prepared by a spin-cast method (ca. 1500 r.p.m.). A dilute polymer solution of $CHCl_3$ (ca. 10^{-6} M, 50 μl) was used. AFM imaging was carried out at 25 ± 1 °C in air. On the other hand, a fast-scanning (high-speed) AFM (FS-AFM) was also conducted for imaging of the structure and dynamics. A FS-AFM (NVB500, Olympus) was modified for a polymer imaging.[27] A cantilever (USC-F1.2-k0.15, NanoWorld AG, Switzerland or OMCL-AC10DS, Olympus) was used. The set point, frame rate, image pixels and the feedback gains were regulated for a video recording. A specimen for FS-AFM imaging was prepared by a similar method of above AFM imaging. Dynamic structure of a polymer chain was observed under *n*-octylbenzene on a mica substrate at 25 ± 1 °C.[28]

RESULTS AND DISCUSSION

The nickel-catalyzed polymerization of the optically active isocyanide monomer comprising quinquethiophene units with two *n*-hexyl chains, **3a**, resulted in the formation of poly-**3a** (Scheme 1). A viscosity of the reaction medium drastically increased as a function of polymerization time, and the initial homogeneous solution finally became a turbid gel. The isolated poly-**3a** had limited solubility in common organic solvents, but was partially soluble in THF and $CHCl_3$. The molecular weight of the soluble part of the obtained polymer was estimated to exceed 1.0×10^6 g mol^{-1} by size-exclusion chromatography (run 1 in Table 1).

The CD and absorption spectra of poly-**3a** were measured in $CHCl_3$ after the solution was passed through a membrane filter with a pore size of 0.45 μm to remove insoluble part of poly-**3a** (Figure 1). For comparison, the spectra of the corresponding monomer, **3a**, are also depicted in Figure 1. The obtained polymer exhibited a characteristic CD in the absorption region of both the polyisocyanide backbone (280–350 nm) and the OT pendant functional group (350–500 nm), whereas the corresponding monomer failed to show any clear CD absorption in either region. According to previous results relating to L-alanine-based polyisocyanides,[13] the positive Cotton effect at ~300 nm suggests that the poly-**3a** backbone formed a right-handed helical conformation. In addition, the clear split-type CD absorption in the region over 350 nm, in which the first Cotton effect at ~470 nm was negative, can be attributed to chiral exciton coupling between the OT pendants. This indicates that the OT pendants within poly-**3a** are arranged in a counterclockwise twisting manner. Consequently, the

CD spectral analysis confirmed that poly-**3a** bearing a quinquethiophene unit successfully formed a preferred-handed helical conformation with a helical array of the functional OT pendants biased by the chirality of the L-alanine residues.

When a small amount of trifluoroacetic acid as a hydrogen bond inhibitor was added to the $CHCl_3$ solution of poly-**3a**, the CD intensity over the entire area was drastically diminished (Figure 2). In agreement with a previously reported result,[13] the preferred-handed helical conformation of poly-**3a** cannot be maintained in the presence of trifluoroacetic acid. Therefore, the successive intramolecular hydrogen-bonding interactions between the neighboring amide groups must play an essential role in the helix formation of poly-**3a** bearing OT pendants.

AFM imaging of poly-**3a** on a mica substrate in air at 25 ± 1 °C was conducted (Figure 3). A network structure was observed, and the individual chain structure was also measured to be 4.4×10^2 nm in length and 1.5 nm in height (Figure 3c). A molecular model of poly-**3a** was constructed by MD method as shown in Figure 4 based on previous reports,[12,14,15] in which a polyisocyanide backbone had a right-handed 4/1 helical conformation. On the basis of the model at

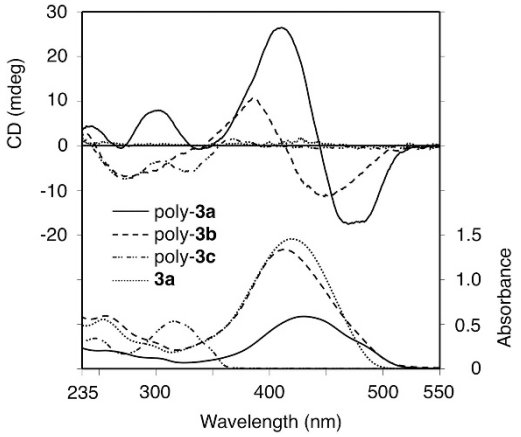

Figure 1 Circular dichroism (CD; upper) and absorption (lower) spectra of poly-**3a**–poly-**3c** and **3a** in chloroform ($CHCl_3$) at 25 °C. Concentrations were adjusted to 3.0×10^{-4} M based on repeating units, and were calculated assuming no insoluble parts.

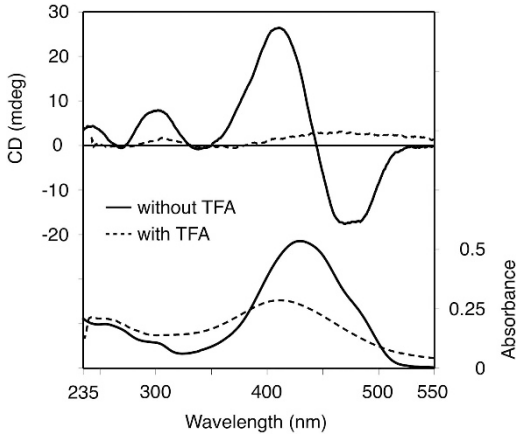

Figure 2 Circular dichroism (CD; upper) and absorption (lower) spectra of poly-**3a** in chloroform ($CHCl_3$; solid line) and $CHCl_3$/trifluoroacetic acid (TFA) (100/0.1, v/v) (dotted line) at 25 °C. Concentrations were adjusted to 3.0×10^{-4} M based on repeating units, and were calculated assuming that there were no insoluble parts.

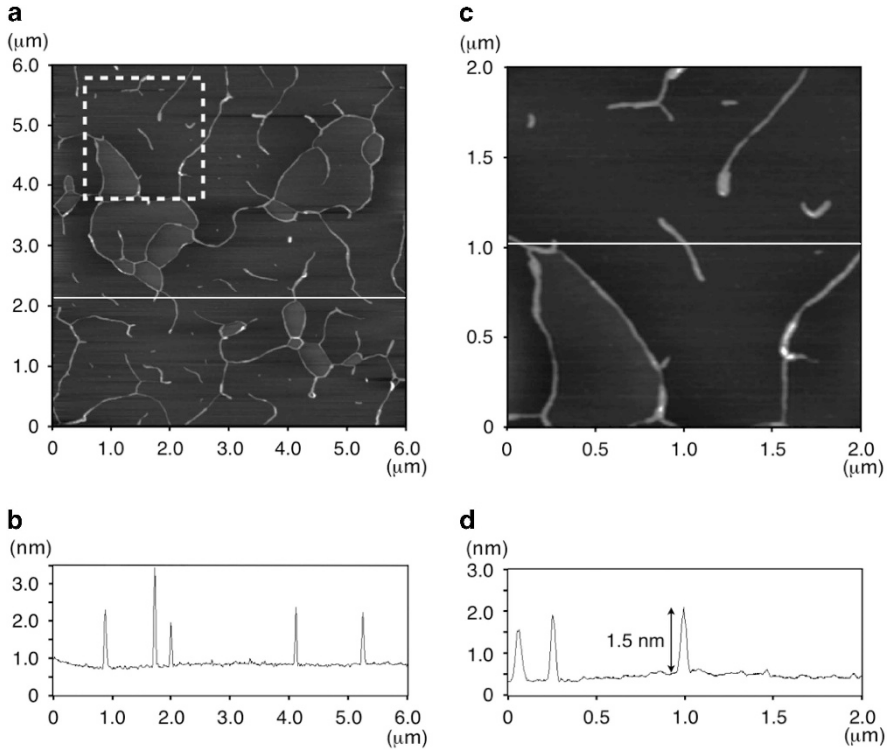

Figure 3 Atomic force microscope (AFM) images of poly-**3a** on mica under air at 25 ± 1 °C. (**a**) The observation area is $6.00 \times 6.00\ \mu m^2$, (**b**) corresponding line profile of image (**a**), (**c**) enlarged AFM image of a dashed square part ($2.00 \times 2.00\ \mu m^2$) in (**a**) and (**d**) corresponding line profile of image (**c**).

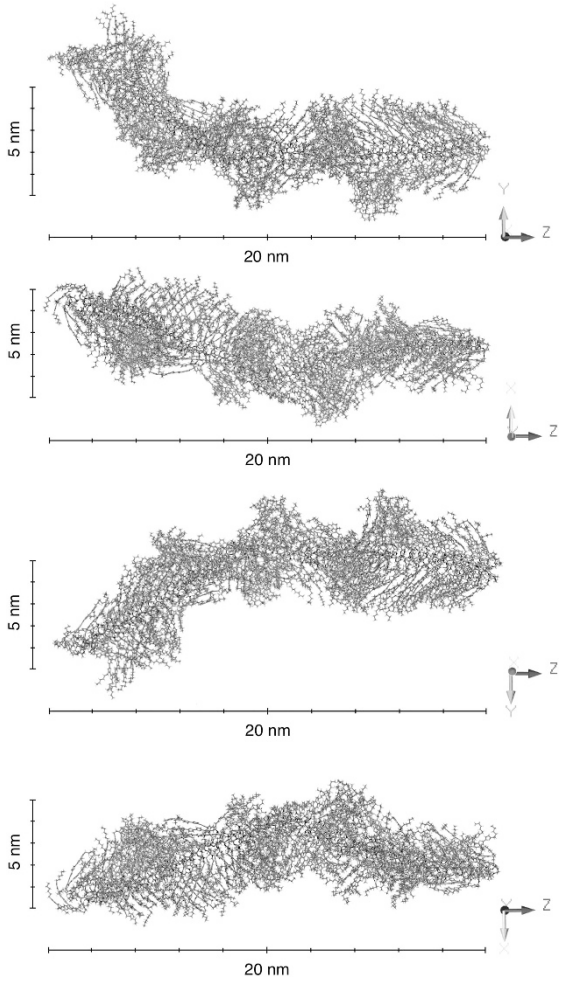

Figure 4 Molecular models of poly-**3a** (200-mer) at 200 ps in molecular dynamics (MD) simulations represented by stick models. In descending order, each model is rotated 90° to the Z axis. A full color version of this figure is available at *Polymer Journal* online.

298K, the chain length of a 200-mer of poly-**3a** was measured as being 20 nm, and the chain width was 2–5 nm because of the structural flexibility. The relative average degree of polymerization of the soluble part of poly-**3a**, as measured by size-exclusion chromatography, was calculated to be 2.7×10^3, although it is a relative value as the polystyrene standard. Accordingly, the average chain length of poly-**3a** was calculated as being 2.7×10^2 nm. From a comprehensive perspective of the size of the isolated structures in the AFM image and the single-molecular size estimated from the combination of the MD simulations and size-exclusion chromatography analytical results, it is concluded that the individual chain in Figure 3 is a single molecule of poly-**3a**. Furthermore, the images suggest that the relatively high-molecular-weight polymers with repeating units in the order of 10^3 are indeed synthesized from **3a** bearing quinquethiophene units. The observed network of μm-length architectures is presumed to be a self-organized aggregate grown selectively in the direction of the main chain. The aggregation architectures may form during the drying process of the dilute polymer solution on the mica substrate rather than in the preparation step of its solution as described in the following section relating to the concentration dependency of the optical properties. Such behavior in AFM observations is consistent with the results of previously reported polyisocyanides.[17,29] In addition, dynamic structure of poly-**3a** was observed by FS-AFM (Supplementary Movie S1).

In sharp contrast to the results of poly-**3a**, the polymerization of the isocyanide monomer **3b** bearing bulky branched alkyl chains at the terminal thiophene ring of the quinquethiophene units progressed homogeneously until complete consumption of **3b** was confirmed. The obtained poly-**3b** exhibited good solubility in THF and $CHCl_3$ without any insoluble moieties. The molecular weight of poly-**3b** was determined to be 0.22×10^6 g mol^{-1} (run 2 in Table 1), an order of magnitude smaller than that of poly-**3a**. This difference in molecular weight was complemented by direct observation, as can be seen in the FS-AFM images (Supplementary Movie S2). During polymerization of the monomer **3b**, the steric hindrance between the branched alkyl chains appears to influence a nickel-catalyzed propagation reactions at the terminal ends.

As shown in Figure 1, the absorption region of the OT pendant in poly-**3b** was shifted by ca. 20 nm toward shorter wavelengths when compared with that in poly-**3a** (Table 1). Because the concentration dependencies were hardly observed under a 10-fold dilute condition (Supplementary Figure S1), the difference in the absorption regions between poly-**3a** and poly-**3b** can be ascribed to the interaction between OT pendants within a single polymer chain, rather than to intermolecular interactions. Hence, adjacent thiophene rings within the OT pendants of poly-**3b** twist to a greater degree and have shortened π-conjugation lengths; this is probably because of the intramolecular steric interaction between the bulky alkyl chains. The dramatic gap in absorption intensities between these polymers results from the fact that poly-**3a** was not completely soluble in $CHCl_3$. In addition, poly-**3b** did not display a positive Cotton peak at 300 nm, and this indicates that the polymer did not form a preferred-handed helical conformation. The CD pattern in the absorption region of the poly-**3b** backbone is quite similar to that of previously reported polyisocyanides with a random conformation.[13] This is further evidence that poly-**3b** did not form a helix formation. Because of the irregular conformation of poly-**3b**, its intensity of the exciton-coupled CD, derived from the OT pendants, was significantly decreased relative to that in poly-**3a**. The weak CD absorption of the OT pendants in poly-**3b** presumably resulted from the successive location of the optically active alanine residues bearing the OT pendants. These results suggest that the alkyl chain far from the isocyano group remotely and sensitively influences not only the polymerizability of the isocyanide monomers but also the helix formation of the obtained polymers.

We also synthesized poly-**3c** bearing a bithiophene pendant with an *n*-hexyl chain that was entirely soluble in THF and $CHCl_3$, and the influence of the number of thiophene rings constituting OT pendants on the higher-order structure formations was investigated. Although the absorption region of the polyisocyanide backbone partly overlapped with that of the bithiophene unit, poly-**3c** did not show a positive CD absorption at ~300 nm and its CD pattern was a similar to that of poly-**3b** with a random conformation, particularly in the region below 300 nm (Figure 1). Therefore, poly-**3c** also seems to exist in a nonhelical conformation. The results demonstrate that the stability of a helical conformation of polyisocyanides bearing a OT pendant is also affected by the number of thiophene rings constituting the OT pendant groups, and that efficient π–π stacking interactions between OT pendants with a larger π-conjugated plane has an important role in the formation of higher-order structures.

CONCLUSIONS

We synthesized a series of L-alanine-based polyisocyanides (poly-**3a**–poly-**3c**) bearing OT pendants, and found that the frameworks of the OT pendants remarkably influenced their chiroptical properties and helix-forming abilities. The polymer possessing quinquethiophene units with two *n*-hexyl chains, poly-**3a**, readily formed a preferred-handed helical conformation with a helical array of the OT pendants biased by the chirality of the L-alanine residues. This study revealed that the simultaneous and effective interactions of the π–π stacking between the OT pendants and the hydrogen bonding between the pendant amide groups are required to arrange the OT pendants into a helically twisted manner along the polyisocyanide backbone. Detailed investigations of the application of these polymers to semiconducting materials are currently in progress and will be reported in due course.

ACKNOWLEDGEMENTS

This work was supported by the Kurata Memorial Hitachi Science and Technology Foundation and the Japan Society for the Promotion of Science (JSPS) KAKENHI Grants-in-Aid for Scientific Research (C), Grant No. 26410129.

1 Gellman, S. H. Foldamers: a manifesto. *Accounts Chem. Res.* **31**, 173–180 (1998).
2 Green, M. M., Park, J.-W., Sato, T., Teramoto, A., Lifson, S., Selinger, R. L. B. & Selinger, J. V. The macromolecular route to chiral amplification. *Angew. Chem. Int. Ed.* **38**, 3138–3154 (1999).
3 Cornelissen, J. J. L. M., Rowan, A. E., Nolte, R. J. M. & Sommerdijk, N. A. J. M. Chiral architectures from macromolecular building blocks. *Chem. Rev.* **101**, 4039–4070 (2001).
4 Fujiki, M. Optically active polysilylenes: state-of-the-art chiroptical polymers. *Macromol. Rapid Commun.* **22**, 539–563 (2001).
5 Hill, D. J., Mio, M. J., Prince, R. B., Hughes, T. S. & Moore, J. S. A field guide to foldamers. *Chem. Rev.* **101**, 3893–4012 (2001).
6 Nakano, T. & Okamoto, Y. Synthetic helical polymers: conformation and function. *Chem. Rev.* **101**, 4013–4038 (2001).
7 Rudick, J. G. & Percec, V. Induced helical backbone conformations of self-organizable dendronized polymers. *Accounts Chem. Res.* **41**, 1641–1652 (2008).
8 Yashima, E., Maeda, K., Iida, H., Furusho, Y. & Nagai, K. Helical polymers: synthesis, structures, and functions. *Chem. Rev.* **109**, 6102–6211 (2009).
9 Nolte, R. J. M. Helical poly(isocyanides). *Chem. Soc. Rev.* **23**, 11–19 (1994).
10 Schwartz, E., Koepf, M., Kitto, H. J., Nolte, R. J. M. & Rowan, A. E. Helical poly (isocyanides): past, present and future. *Polym. Chem.* **2**, 33–47 (2011).
11 Cornelissen, J. J. L. M., Fischer, M., Sommerdijk, N. A. J. M. & Nolte, R. J. M. Helical superstructures from charged poly(styrene)-poly(isocyanodipeptide) block copolymers. *Science* **280**, 1427–1430 (1998).
12 Cornelissen, J. J. L. M., Donners, J. J. J. M., Gelder, R., Graswinckel, W. S., Metselaar, G. A., Rowan, A. E., Sommerdijk, N. A. J. M. & Nolte, R. J. M. β-Helical polymers from isocyanopeptides. *Science* **293**, 676–680 (2001).
13 Cornelissen, J. J. L. M., Graswinckel, W. S., Rowan, A. E., Sommerdijk, N. A. J. M. & Nolte, R. J. M. Conformational analysis of dipeptide-derived polyisocyanides. *J. Polym. Sci. A Polym. Chem.* **41**, 1725–1736 (2003).
14 Gowda, C. M., van Eck, E. R. H., van Buul, A. M., Schwartz, E., van Pruissen, G. W. P., Cornelissen, J. J. L. M., Rowan, A. E., Nolte, R. J. M. & Kentgens, A. P. M. Direct backbone structure determination of polyisocyanodipeptide using solid-state nuclear magnetic resonance. *Macromolecules* **45**, 2209–2218 (2012).
15 Schwartz, E., Liegeois, V., Koepf, M., Bodis, P., Cornelissen, J. J., Brocorens, P., Beljonne, D., Nolte, R. J., Rowan, A. E., Woutersen, S. & Champagne, B. Beta sheets with a twist: the conformation of helical polyisocyanopeptides determined by using vibrational circular dichroism. *Chem. Eur. J.* **19**, 13168–13174 (2013).
16 De Witte, P. A. J., Hernando, J., Neuteboom, E. E., van Dijk, E. M. H. P., Meskers, S. C. J., Janssen, R. A. J., van Hulst, N. F., Nolte, R. J. M., García-Parajó, M. F. & Rowan, A. E. Synthesis and characterization of long perylenediimide polymer fibers: from bulk to the single-molecule level. *J. Phys. Chem. B* **110**, 7803–7812 (2006).
17 Finlayson, C. E., Friend, R. H., Otten, M. B. J., Schwartz, E., Cornelissen, J. J. L. M., Nolte, R. J. M., Rowan, A. E., Samorì, P., Palermo, V., Liscio, A., Peneva, K., Müllen, K., Trapani, S. & Beljonne, D. Electronic transport properties of ensembles of perylene-substituted poly-isocyanopeptide arrays. *Adv. Funct. Mater.* **18**, 3947–3955 (2008).
18 Palermo, V., Otten, M. B. J., Liscio, A., Schwartz, E., de Witte, P. A. J., Castriciano, M. A., Wienk, M. M., Nolde, F., De Luca, G., Cornelissen, J. J. L. M., Janssen, R. A. J., Müllen, K., Rowan, A. E., Nolte, R. J. M. & Samorì, P. The relationship between nanoscale architecture and function in photovoltaic multichromophoric arrays as visualized by Kelvin probe force microscopy. *J. Am. Chem. Soc.* **130**, 14605–14614 (2008).
19 Dabirian, R., Palermo, V., Liscio, A., Schwartz, E., Otten, M. B. J., Finlayson, C. E., Treossi, E., Friend, R. H., Calestani, G., Müllen, K., Nolte, R. J. M., Rowan, A. E. & Samorì, P. The relationship between nanoscale architecture and charge transport in conjugated nanocrystals bridged by multichromophoric polymers. *J. Am. Chem. Soc.* **131**, 7055–7063 (2009).
20 Foster, S., Finlayson, C. E., Keivanidis, P. E., Huang, Y.-S., Hwang, I., Friend, R. H., Otten, M. B. J., Lu, L.-P., Schwartz, E., Nolte, R. J. M. & Rowan, A. E. Improved performance of perylene-based photovoltaic cells using polyisocyanopeptide arrays. *Macromolecules* **42**, 2023–2030 (2009).
21 Schwartz, E., Lim, E., Gowda, C. M., Liscio, A., Fenwick, O., Tu, G., Palermo, V., de Gelder, R., Cornelissen, J. J. L. M., Van Eck, E. R. H., Kentgens, A. P. M., Cacialli, F., Nolte, R. J. M., Samori, P., Huck, W. T. S. & Rowan, A. E. Synthesis, characterization, and surface initiated polymerization of carbazole functionalized isocyanides. *Chem. Mater.* **22**, 2597–2607 (2010).
22 Mishra, A., Ma, C.-Q. & Bäuerle, P. Functional oligothiophenes: molecular design for multidimensional nanoarchitectures and their applications. *Chem. Rev.* **109**, 1141–1276 (2009).
23 Takagi, K., Nobuke, K., Nishikawa, Y. & Yamakado, R. Synthesis and optical properties of poly(p-benzamide)s bearing oligothiophene on the amide nitrogen atom through an alkylene spacer. *Polym. J.* **45**, 1171–1176 (2013).
24 Morisaki, Y., Inoshita, K., Shibata, S. & Chujo, Y. Synthesis of optically active through-space conjugated polymers consisting of planar chiral [2.2]paracyclophane and quaterthiophene. *Polym. J.* **47**, 278–281 (2015).
25 Zhang, L., Colella, N. S., Cherniawski, B. P., Mannsfeld, S. C. & Briseno, A. L. Oligothiophene semiconductors: synthesis, characterization, and applications for organic devices. *ACS Appl. Mater. Inter.* **6**, 5327–5343 (2014).
26 Shinohara, K., Suzuki, T., Kitami, T. & Yamaguchi, S. Simultaneous imaging of the structure and fluorescence of a supramolecular nanostructure formed by the coupling of f action vessels for cascade reactions.. ecular interaction. *J. Polym. Sci. A Polym. Chem.* **44**, 801–809 (2006).
27 Shinohara, K. Dynamic analysis method for polymer chain, manufacturing method for polymer, polymer, manufacturing method for synthetic polymer, and synthetic polymer, WO/2014/104172 (3 July 2014).
28 Shinohara, K., Kodera, N. & Oohashi, T. Single-molecule imaging of photodegradation reaction in a chiral helical π-conjugated polymer chain. *J. Polym. Sci. A Polym. Chem.* **48**, 4103–4107 (2010).
29 Cornelissen, J. J. L. M., Graswinckel, W. S., Adams, P. J. H. M., Nachtegaal, G. H., Kentgens, A. P. M., Sommerdijk, N. A. J. M. & Nolte, R. J. M. Synthesis and characterization of polyisocyanides derived from alanine and glycine dipeptides. *J. Polym. Sci. A Polym. Chem.* **39**, 4255–4264 (2001).

Supplementary Information accompanies the paper on Polymer Journal website (http://www.nature.com/pj)